2018 IEEE 15th International Conference on Mobile Ad-hoc and Sensor Systems

Using Wireless Tags to Monitor Bodily Oscillation

Youlin Zhang* Shigang Chen* You Zhou*‡ Yuguang Fang†
*Department of Computer & Information Science & Engineering, University of Florida, Gainesville, FL 32611, USA,
†Department of Electrical & Computer Engineering, University of Florida, Gainesville, FL 32611, USA,
‡Google Inc., 1600 Amphitheatre Parkway, Mountain View, CA, USA
Email: {youlin, sgchen}@cise.ufl.edu, {youzhou}@google.com, {fang}@ece.ufl.edu

***Abstract*—Traditional systems for monitoring and diagnosing patients' health conditions often require either dedicated medical devices or complicated system deployment, which incurs high cost. The networking research community has recently taken a different technical approach of building health-monitoring systems at relatively low cost based on wireless signals. However, the RF signals carry various types of noise and have time-varying properties that often defy the existing methods in more demanding conditions with other body movements, which makes it difficult to model and analyze the signals mathematically. In this paper, we design a novel wireless system using commercial off-the-shelf RFID readers and tags to provide a general and effective means of measuring bodily oscillation rates, such as the hand tremor rate of a patient with Parkinson's disease. Our system includes a series of noise-removal steps, targeting at noise from different sources. More importantly, it introduces two sliding window-based methods to deal with time-varying signal properties from channel dynamics and irregular body movement. The proposed system can measure bodily oscillation rates of multiple persons simultaneously, even when the individuals are moving. Extensive experiments show that our system can produce accurate measurement results with errors less than 0.3 oscillations per second when it is applied to monitor hand tremor.**

I. Introduction

Health-monitoring systems are now widely used in monitoring and diagnosing various health issues. For example, sensing the respiration rate can help monitor sleep apnea and chronic obstructive pulmonary disease; measuring the hand tremor rate can help monitor the conditions of a patient with Parkinson's Disease (PD). Traditional health-monitoring systems [1]–[3] require either dedicated medical devices or complicated system deployment, which incurs high cost. The networking research community recently takes a different design path to utilize wireless signals for building health-monitoring systems at low cost.

Radio frequency (RF) based technologies for monitoring human activities [4]–[8] have drawn much attention from the research community recently. For example, Patwari et al. [4] extract the coarse-grained Received Signal Strength (RSS) from the wireless sensor nodes to estimate the human respiration rate. This approach requires deployment of multiple (more than 12) dedicated sensor nodes, which is cumbersome and resource costly. UbiBreathe [7] estimates the human respiration rate by measuring the RSS of WiFi signals. It can produce more accurate measurement results than the above sensor-based system. However, it requires a user to lay down and place a mobile device on the chest, which is much inconvenient; otherwise, if the device is placed by the side of the person, the accuracy of the measurement results significantly degrades. The system designed by Liu et al. [5] provides a device-free solution for tracking vital signs during sleep. It extracts the fine-grained Channel State Information (CSI) [9] using WiFi devices to track the breathing rate and the heart-beat rate of a person in bed. Again, the person has to stay still in order to avoid introducing disturbance to WiFi signals. Therefore, the system cannot support continuous monitoring in day time when the person may move around, which is a condition assumed in this paper as hand tremor can come and go, and may happen at any time. Another limitation is that it can simultaneously monitor two persons at most. The designs of the above systems are mostly geared towards measuring respiration rates under static, restrained settings, not for tremor rates, which are much faster at multiple ticks per second and are measured under dynamic settings allowing free movement.

To address the limitation of the prior systems, we propose and build an RFID-based easily deployable wireless system for measuring hand tremor rate in dynamic settings where wireless signals are not perfectly periodic. RFID technologies have gained popularity in recent years. Numerous applications have been developed, including inventory control, supply chain management, product tracking, and indoor localization [10]–[16]. A typical RFID system consists of a reader and many tags, forming a simple reader-tag wireless network. Tags are very cheap and convenient to deploy, which helps promote their widespread usage. With this advantage, the proposed system is unique with its capability of accurately measuring hand tremor rates of multiple persons, even when they are moving around. While this paper focuses on hand tremor rate, the signal processing techniques in our paper are generic and our system can be extended measure other bodily oscillation rate as well by attaching an RFID tag to body part under measurement or the immediate clothing to that body part. Because an RFID reader can easily distinguish the backscatter signals from multiple tags, our system is able of simultaneously measuring the oscillation rates of different tags attached to multiple persons or different places on the same person. Using only commercial off-the-shelf RFID readers/tags, the system is designed to work in either hospital/clinic settings where multiple patients can be monitored simultaneously or home settings where patients may borrow mobile readers from hospitals to perform continuous monitoring with the comfort at home. Tags cost as little as a dime a piece. They can be tossed away after being used, which is desirable in medical

2155-6814/18/$31.00 ©2018 IEEE
DOI 10.1109/MASS.2018.00042

context.

Our system measures the phase values of RF signals in tag-reader communication and estimates oscillation rate based on the periods in phase change. An RFID reader can measure two important properties of the RF signals: RSS values and phase values. The RSS values of weak RFID signals do not work well for our purpose due to the following reasons: On the one hand, oscillation on human body is a small movement, which produces very small changes in RSS. On the other hand, the measurement of RSS by a commercial reader is noisy and coarse, with a resolution of 0.5 dB [17], so that the small bodily movement will not even affect the reported RSS values. In contrast, the phase resolution by a commercial reader is high, reaching 0.0015 rad [17], which translates to a spatial resolution of 0.04 centimeters. Such a fine spatial resolution enables us to catch slight oscillations such as hand tremor.

There are several technical challenges in the design of our system: First, the phase values measured by a reader are not well-shaped due to environmental noise, device imperfection, and measurement errors. Second and more importantly, unlike machine-produced vibrations, human's bodily oscillation is time-variant. The irregularity in oscillation makes it difficult to model precisely or analyze mathematically. Third, when monitoring is performed at a relaxed setting where patients can move around, it introduces unpredictable changes in the measured phase values. We develop a series of methods to handle the above challenges by removing noises from various sources and by introducing two sliding window-based methods to process time-varying phase data, from which we reveal the oscillation pattern and derive the oscillation rate accurately.

We have built a prototype system for performance evaluation, which shows that the proposed system can accurately estimate hand tremor rate under a variety of settings: when measuring the hand tremor rate of a single person who sits, the average error is 0.11 tick per second (*tps*); when simultaneously measuring the hand tremor rates of four persons who sit, the average error is just 0.14 *tps*; when simultaneously measuring the hand tremor rates of four moving persons, the average error is 0.26 *tps*.

II. Related Work

Research in patient activity monitoring can be classified into three categories: dedicated sensor based, smart phone and wearable device based, and RF signal based.

Traditional methods for activity monitoring use dedicated sensors. For example, Patel, et al. [2] leverage wearable sensors to monitor Parkinson's disease (PD) with the collected data relayed to a remote clinical site via a web-based application. Albani et al. [3] use Electromyography (EMG) to study tremor in PD, detect basic body postures, and study gait in PD patients. Polysomnography (PSG) [1] attaches multiple sensors to a patient to monitor human health conditions including respiration rate, heart beat rate, eye movements and muscle activity. This kind of technique requires specialized devices, which can make people uncomfortable in use. Besides, additional network infrastructure is needed for collecting and processing the data.

Recent research exploits embedded functions of smart phones and wearable devices such as accelerometers and GPS to monitor patient activities [18], [19]. For example, Hao et al. [18] use the microphone of a smart phone to measure sleep quality, with detection of sleep events such as body movement, couch and snore. But it cannot quantitatively measure the bodily oscillation rate of human bodies such as hand tremor rate. PERFORM [19] proposes an intelligent close-loop system which integrates four wearable sensors to monitor activities of the PD patients. These sensors are more costly and less comfortable to wear than RFID tags, which are small, thin, flexible and easily attachable to body or cloth.

Most related to our work is the RF signal based approach for human activity monitoring. Some systems use Doppler radars [20], ultra-wideband (UWB) radars [21], or frequency modulated carrier waves (FMCW) radars [6]; others rely on measurement of received signal strength (RSS) [4], [7], channel state information (CSI) [5], [8], or phase values [12], [22]. Specifically, the systems [4], [6], [21] that require specialized devices such as Doppler radars, UWB radars or wireless sensors incur high cost, and they require trained personnel to deploy. While UbiBreathe [7] improves accuracy over [4] in estimating respiration rate based on RSS measurements, it achieves its best accuracy with an error smaller than 1 breath per minute (*bpm*) when it places a mobile device on a patient's chest. Under the device-free mode, it has an error greater than 1.5 *bpm*, and this mode imposes that the patient being monitored has to stay in the line of sight between a wireless transmitter and a receiver. Liu et al. [5] propose a system utilizing fine-grained CSI for measuring a patient's breathing rate and heart rate. Their method is device-free but relies on relative positions of the patient and WiFi devices used. In addition, the system cannot be applied to more than two persons simultaneously. Wang et al. [8] propose another WiFi-based breathe monitoring system that improves over [5], [7]. This system uses WiFi Fresnel Zone to monitor human respiration. It can accurately measure human respiration rate under arbitrary body orientation and posture. It also can only monitor two persons at once. TagBreathe [12] uses the phase values of RFID tags to monitor respiration rate and can support multiple users. Like [5], [8], it does not consider dynamic settings that allow patients to move around for continuously monitoring in daily-life activities. The design of the above systems heavily relies on positioning of devices and patients. Also related is Tagbeat [22], which measures the rotation period of a centrifuge machine. Its method is applicable to measuring wind speed, monitoring centrifugation, and troubleshooting engine [22]. It requires static and steady conditions where the mechanical vibration of an object produces near-perfect periodic cures in wireless signals, which are time-invariant in the spectrum domain. This is a condition that does not hold for oscillations in human body such as hand tremor that carries inherent irregularity in both frequency and magnitude.

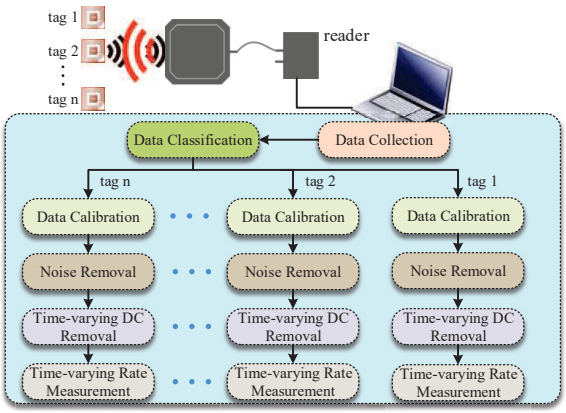

Fig. 1: Our system architecture.

III. System Overview

The goal of our system is to measure the bodily oscillation rate, using hand tremor as a study case. The system deployment is simple: an RFID tag is attached to the hand (or other body part) under monitoring. An RFID reader is deployed in the room to continuously measure the phase values of the wireless signals backscattered from the tag. The patient is allowed to move within the coverage area of the reader. Multiple tagged patients can be monitored simultaneously.

The basic idea behind our approach is that when a hand attached with an RFID tag shakes, this oscillation will introduce a periodic component in the reported phase values. Therefore, we can analyze the collected phase values and extract this periodic pattern. Once the oscillation pattern is captured, the hand tremor rate can be estimated.

Our system in Fig. 1 consists of six modules: Data Collection, Data Classification, Data Calibration, Noise Removal, Time-varying DC Removal and Time-varying Rate Measurement. All these modules can be implemented on a laptop connected to an RFID reader. Assume we have n people to be monitored, each of which is attached with a tag on his hand. Our system first collects the phase values of the tags by an RFID reader. The collected data is then processed by the Data Classification module, which classifies the data into different groups based on the reported tag IDs. After Data Classification, the data of each group will be processed separately by the Data Calibration module, the Noise Removal module, the Time-varying DC Removal module, and the Time-varying Rate Measurement module, which outputs the oscillation rate. The details of these modules will be elaborated in Section IV.

IV. System Design

In this section, we present the functional details of our system on how the phase values are processed step by step to produce an estimated oscillation rate. In the sequel, we use the terms, "tremor" and "tremble", exclusively for hands, and the terms, "static", "moving", and "movement", for other larger bodily movement such as moving an arm or walking.

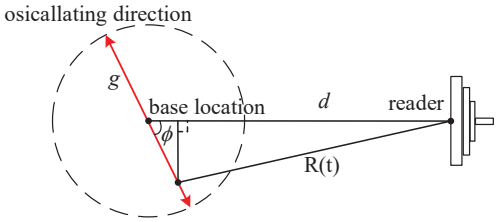

Fig. 2: Hand tremor model.

For example, when we say "hand tremor rate of one *static* person", the word "static" means that the person does not have any other bodily movement except that one of his hands trembles. With "hand tremor rate of one *moving* person", we mean that the person may be waving his arm or walking when one of his hands trembles. For the cases of measuring hand tremor rates of multiple persons, we allow the individuals to move as they wish.

A. Time-varying Properties

Before we elaborate the design of our system, we first mathematically analyze the time-varying properties of a tag's phase values when it is attached to a trembling hand. We begin by examining the ideal motion in [12] where a tag oscillates in perfect harmonic motion along the direction of the double arrow in Fig. 2. The middle point of the double arrow is called the base location of oscillation. Let d be the distance between the base location and the reader's antenna, ϕ the acute angle between the line of oscillation and the line from the reader to the base location, r the rate of oscillation, and g the magnitude of oscillation.

Consider harmonic motion in which the distance from the tag to the base location can be modeled as $g\sin(2\pi rt)$. From the figure, it is easy to see that the tag-reader distance $R(t)$ is

$$R(t) = \sqrt{(d - g\sin(2\pi rt)\cos\phi)^2 + (g\sin(2\pi rt)\sin\phi)^2}, \tag{1}$$

which has a period of $\frac{1}{r}$. As the tag-reader distance changes over time, it creates a phase shift in the backscattered signal received by the reader. Today's reader can typically produce around 40 phase samples at random times based on an arbitration protocol that resolves collision when multiple tags are present [23]. Each sample includes the tag ID, the time when the sample is taken, and the phase. For an oscillation characterized by (1), the phase $\theta(t)$ can be modeled as

$$\theta(t) = \theta_0 + 2\pi\frac{2R(t)}{\lambda} \mod 2\pi \tag{2}$$

where an offset θ_0 is introduced by the hardware, λ is the wavelength of the RF waves, and the total distance travelled by the waves from the reader to the tag and back to the reader is $2R(t)$.

Clearly, $\theta(t)$ is a periodic curve, with a period of $\frac{1}{r}$. It has been shown in [22] that a periodic phase curve can be approximately recovered from discrete random samples (produced by the reader) using the method of compressive sensing. The assumption is that the curve has nearly perfect

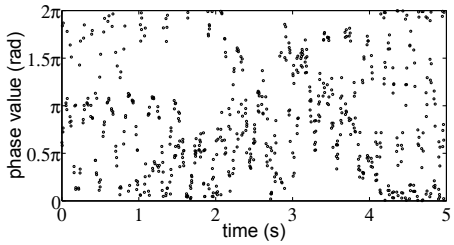

Fig. 3: Phase samples when four people move with their hands trembling.

periods where the phase repeats the same values in each period, as is the case of machine-induced vibrations studied in [22] and also is the case in the ideal model of (1)-(2) above.

However, this paper studies the oscillations produced by human body, which have time-varying properties that break the above assumption. For example, consider that a tagged hand trembles. The oscillation rate r may change over time. The tremor magnitude g may also change over time. The person may walk around, and therefore d and ϕ change over time. In this situation, $\theta(t)$ is no longer a periodic curve in the mathematical sense. It can be a complex, non-repeating curve that shows oscillation but defies the use of compressive sensing and other methods that assume mathematically periodic curves. To reflect the time-varying properties, the model of (1)-(2) has to be rewritten as

$$\begin{aligned} R(t) =& \sqrt{(d(t) - g(t)\sin(2\pi r(t)t)\cos\phi(t))^2} \\ & \overline{+(g(t)\sin(2\pi r(t)t)\sin\phi(t))^2} \\ \theta(t) =& \theta_0 + 2\pi\frac{2R(t)}{\lambda} + \varepsilon \qquad \mod 2\pi \end{aligned} \tag{3}$$

where ε is an error caused by environmental noise. Such a model is hard to analyze using the traditional methods. Therefore, new ways must be invented to find the oscillation rate not based on model analysis but based directly on the time-varying phase samples. Before explaining the details of our approaches, we first describe how we collect data from users.

B. Data Collection and Classification

Suppose we have n users, each of which is attached with an RFID tag to a finger and each tag has a unique ID. The reader continuously interrogates the tags, which respond by backscattering the RF signals from the reader. The reader performs a collision-resolving arbitration protocol [23] that allows it to communicate with the tags in turn, collecting the individual tag IDs and the associated physical-layer signal properties such as phase shift and received signal strength.

Fig. 3 shows an example of the collected phase values from four moving people when their hands (tags) are trembling. In this figure, each point represents a phase sample we have collected. Since the four tags' phase values are randomly sampled and mixed together in the data, we cannot observe any periodic pattern. Fortunately, the phase samples are collected together with tag IDs, which allows us to easily separate the data into four groups, one for each tag. We can then process each group of data at a time to obtain the hand tremor rate of one person. In the following, we will focus on the data from one person.

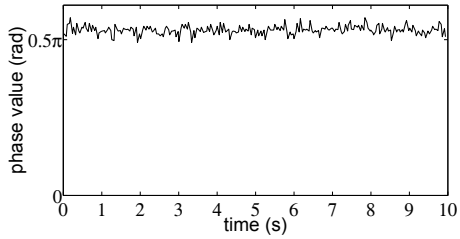

(a) phase samples when a person stays still without hand tremor.

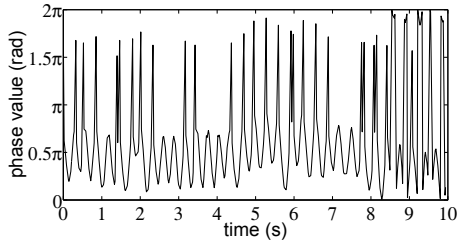

(b) phase samples when a person has one hand trembling.

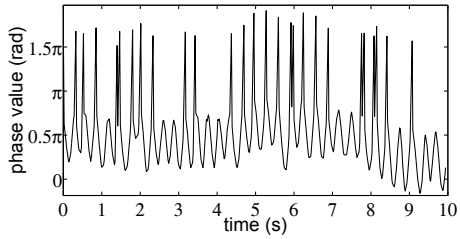

(c) phase samples after data calibration.

Fig. 4: Phase samples produced by a reader for a tagged person.

C. Data Calibration and Noise Removal

Consider the set of phase samples produced by an RFID reader for a specific tag. These samples are inherently noisy due to environment interference and product properties [17]. Fig. 4a shows the phase samples recorded by the reader from one tagged person whose hand stays still; refer to Section V for details of the testbed. Note that we connect the adjacent phase values in the figure to show a phase curve with spikes whose tips are where the phase samples locate. The phase curve stays largely a constant with small random noise fluctuations.

Fig. 4b shows the phase samples when the person emulates hand tremor by shaking one hand while sitting by a desk without other bodily movement. The curve in the figure is noisy. The time-varying noise is caused by various factors, including device properties and fluctuations in the distance between the reader and the base location of the tag, in the

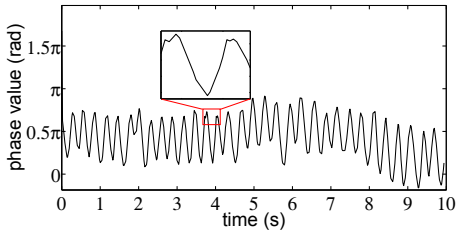

Fig. 5: Phase values from a single static person after spikes are removed.

oscillation rate, and in the oscillation magnitude. Simply applying a low pass filter will not work well. Although it can remove high-frequency noise (such as white noise from the environment), as we will show, much of the noise in our measurement is not of high frequency, which makes the low pass filter ineffective.

Our first observation is that, when the tag moves to a location where the true phase value is close to a multiple of 2π's, as the noise pushes it back and forth around this multiple, the modulo operation in (2) may cause 2π jumps up or down in the reported phase samples. Such large errors are evident in Fig. 4b between 8 sec to 10 sec. To calibrate the phase samples, we enforce continuity in phase changes. If there is a sudden change of about 2π between two consecutive phase values, we know that it is caused by the modulo operation. In this case, we need to remove the sudden 2π change to ensure the continuity between the two phase values. After data calibration, the phase curve becomes Fig. 4c.

Second, not all noise in the phase curve is caused by modulo operation. Tags are very cheap hardware, and there is device imperfection [17], with isolated π shift in some reported phase values, as we have observed in our experiments using different tags. For example, in Fig. 4c, as the basic shape of the phase curve fluctuates between 0 and π, there are spikes of magnitude π into the range of $[\pi, 2\pi)$. In this experiment, the operating frequency is 920 MHz, which means a wavelength of about 32.6 cm. The sampling rate for phase values is around 40 samples per second. The magnitude of hand tremor is smaller than half of a wavelength, which means it is not possible for two consecutive phase-value samples to be apart by π. Therefore, as another noise removal operation, whenever we see a phase jump of more than π between two consecutive phase values, we will reduce the second value by π. After noise removal, the phase curve becomes Fig. 5.

Third, after removing the noise caused by modulo operation and device imperfection, we observe that there is still undesired noise in the data. The remaining noise comes from the environmental interference and can degrade the performance of our method for measuring the oscillation rate based on the number of peaks (or valleys) in the phase curve. As we zoom in to see the details in Fig. 5, there are some small unexpected peaks (called *false peaks*) in the curve that will interfere with our measurement.

Thus we adapt a wavelet based denoising algorithm [24] in

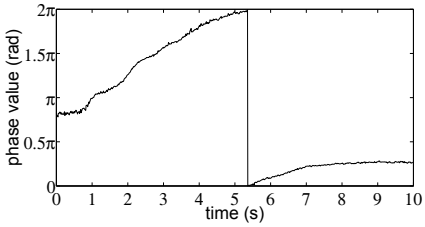

(a) phase samples when a person moves without hand tremor.

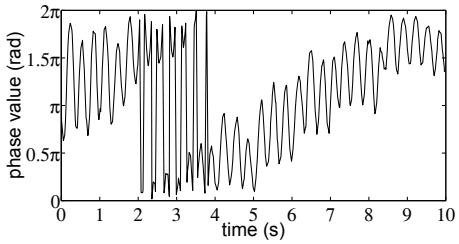

(b) phase samples when a person moves with one hand trembling.

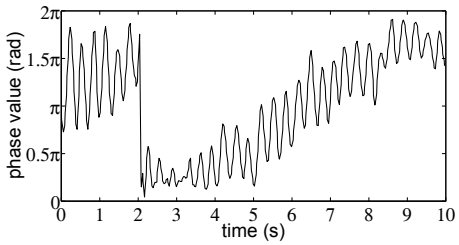

(c) phase samples after noise is removed.

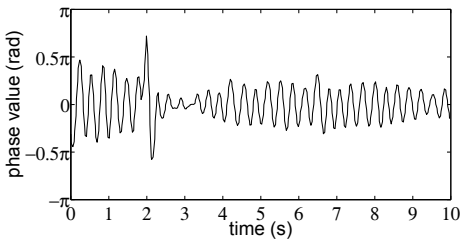

(d) phase samples after time-varying DC is removed.

Fig. 6: Sliding window-based approach for removal of time-varying DC.

our context to remove noise in the phase curve. Traditional methods that use a low (or band) pass filter with cut-off frequency cannot effectively deal with this problem, because the noise may be in the band of the signals, for example, when it is created due to the tagged person's other movement (such as waving arms).

Finally, we reconstruct the signal without noise. We denote the set of phase samples after the above noise removal as Θ^*.

D. Time-varying DC Removal

There exists a time-varying Direct Current (DC) component in the curve, which is partially resulted from the instability of hand when it trembles: Suppose trembling is a cyclic motion around the base location of a hand. Even for a static person without large bodily movement of walking or arm waving, the base location of the hand may still shift slightly over time. If the person actually moves around, the time-varying DC component will be more significant. Fig. 6a shows the phase samples measured in an experiment where a person walks. As the person moves without his hand trembling, the phase value changes steadily, in addition to small high-frequency fluctuations due to environmental noise. When the curve reaches 2π, it will drop to zero due to the modulo operation. Fig.6b shows the phase samples taken when the person moves with his hand trembling. The phase shift is caused by a combination of hand tremor and the person's moving. In addition, when closing to the boundary of 2π or zero, any instability in measurement will cause 2π swings in the module operation, which is evident between 2 to 4 seconds in the plot. Fig. 6c shows the phase values after data calibration (spike removal) and noise removal. Comparing this plot with Fig. 4b, we can see that a person's movement introduces a much greater, time-varying DC component in the phase curve. More significantly, alongside the DC component, there are false peaks (between 2 to 4 seconds) that are not eliminated by the noise removal module, possibly because this noise's frequency is too close to the rate under measurement. Fortunately, we find that by removing the time-vary DC component, we can also remove this noise.

We model the phase sample $\theta(t) \in \Theta^*$ after noise removal as

$$\theta(t) = a + M(t) + \hat{\theta}(t), \tag{4}$$

where a is a constant DC component which is dependent on the initial distance between the tag and the reader's antenna, as well as hardware properties, $M(t)$ is a time-varying DC component due to the shift of the hand's base location, and $\hat{\theta}(t)$ is the oscillating component caused by the hand trembling around the base location. We want to approximately remove $a + M(t)$ from the samples $\theta(t)$ to find the values of $\hat{\theta}(t)$. If trembling is steady as a harmonic motion, $\hat{\theta}(t)$ can be modeled by (3). But in real life, a hand may tremble with time-varying magnitude and rate.

A naive approach of removing DC is to subtract $\theta(t)$ by the global mean of the phase samples. However, this approach does not work well since it will only transpose the phase curve along the vertical axis. We propose a sliding window-based approach that computes a local mean within a sliding window for DC removal. The local mean $l(t)$ at time t within window $[t - \frac{W}{2}, t + \frac{W}{2})$ is defined as

$$l(t) = \frac{1}{W}\int_{t-\frac{W}{2}}^{t+\frac{W}{2}} \theta(t')dt' = \frac{1}{W}\int_{t-\frac{W}{2}}^{t+\frac{W}{2}} [a + M(t') + \hat{\theta}(t')]dt', \tag{5}$$

where W is the size of the window. Within a small time window, we assume $M(t')$ is approximately a linear function and $\theta(t')$ is approximately a periodic function. For example, consider a patient walks around indoor with a hand trembling. Within a time frame of a few seconds, the patient is *likely* to be moving along a line. Even though the patient will make turns, as long as the assumption is roughly satisfied for most such time windows, our approach will work well overall. With the above approximations, we have

$$l(t) \approx a + M(t) + \frac{1}{W}\int_{t-\frac{W}{2}}^{t+\frac{W}{2}} \hat{\theta}(t')dt', \tag{6}$$

Note that $M(t)$ is the mean of $M(t')$ in the window $t' \in [t - \frac{W}{2}, t + \frac{W}{2})$. By definition, $\hat{\theta}(t')$ is the oscillating curve after the DC component is removed. Hence, its integral over each period is zero. When W is much larger than the period length, the value of $\frac{1}{W}\int_{t-\frac{W}{2}}^{t+\frac{W}{2}} \hat{\theta}(t')dt'$ becomes insignificant when comparing with the magnitude of the $\hat{\theta}(t')$ curve. Hence, we have

$$l(t) \approx a + M(t), \tag{7}$$

which is exactly what we want to remove as the time-varying DC component. We can approximately compute the value of $l(t)$ — thus the value of $a + M(t)$ — from (5) based on the phase samples taken in the time window $[t - \frac{W}{2}, t + \frac{W}{2})$. Let $S(t) \subset \Theta^*$ be the subset of phase samples in this window. For each sample $\theta(t')$ taken at a specific time t', let $\Delta(t')$ be the time interval from this sample to the next sample. We approximate the integral in (5) with discrete samples as follows:

$$l(t) = \frac{1}{W}\sum_{\theta(t')\in S(t)} \theta(t') \times \Delta(t'), \tag{8}$$

where $S(t)$ and $\Delta(t')$, $\forall\theta(t') \in S(t)$, can be easily found from the full set Θ^* of phase samples.

The exact value of W should be determined based on the application context. It should be small enough such that $M(t)$ is likely to be linear within a time window, and it should be significantly larger than the oscillation period. To measure the hand trembling rate of a patient indoor, a few seconds should be appropriate. After the local mean $l(t)$ is computed, we subtract it from $\theta(t)$ as follows

$$\hat{\theta(t)} = \theta(t) - l(t), \quad \forall\theta(t) \in \Theta^*. \tag{9}$$

The set of resulting phase values is denoted as $\hat{\Theta}$. For mathematical rigor, we point out that additional phase samples should be taken during a period of $\frac{\max\{W,\hat{W}\}}{2}$ preceding the first sample in Θ^* and a period of the same length after the last sample in Θ^*, where $\hat{W}$ is the width of another sliding window introduced later.

By applying a sliding window step by step over the whole curve, we are able to remove the time-varying DC, as shown in Fig. 6d, which characterizes the phase shift due to hand tremor alone. Most false peaks between 2 and 4 seconds in Fig. 6c are also removed.

(a) reader and antenna

(b) RFID tag

Fig. 7: Experiment setup.

E. Time-varying Oscillation Rate

Once the phase curve of pure hand tremor is produced, we proceed with tremor period identification and oscillation rate measurement. Based on the periodic pattern (demonstrated by Fig. 6d), we identify the peaks (or valleys) on the phase curve, and use the inter-peak distances to estimate the expected tremor period and then compute the oscillation rate. A simple algorithm for identifying peaks is to compare each phase value with its predecessor and the successor on the curve. (Note that even though the phase curve is shown as a continuous curve, it is in fact constructed by connecting the sample phase values.) If a phase value is greater than both the predecessor and the successor, we treat it as a peak.

After we identify all the peaks on the phase curve, we obtain an estimation p of the expected tremor period by taking an average. We denote the n measured peak-to-peak intervals as $\{t_1, t_2, ..., t_i, ..., t_n\}$. The estimation is given as follows:

$$p = \frac{\sum_{i=0}^{n-1} t_i}{n}. \tag{10}$$

With the value of p estimated from the above formula, the oscillation rate of hand tremor can be computed as $1/p$ *tps*.

V. Implementation

We have implemented a prototype of our system as shown in Fig. 7. The system setup is given as follows.

RFID Reader: We use one commercial ImpinJ Speedway R420 reader [17] without any modifications on hardware or software. The reader operates within a frequency range $920 \sim 925$ MHz, as specified by the EPC C1G2 standard [23]. It provides four RP-TNC ports and thus can support up to four antennas. A GPIO Adapter [17] can be exploited to extend the number of connected antennas to 32, which significantly expands the coverage area of the reader. In our experiments, one Laird S9028PCLJ circular polarized antenna [25] as shown in Fig. 7a is sufficient to cover our office area, where the experiments are performed.

RFID Tags: We adopt widely-used Alien Squiggle UHF RFID tags [26] whose dimensions are $1.752'' \times 0.409''$. They have an operation range up to 11 $meters$. Those passive tags harvest energy from the RF signals emitted from the antenna. A tag is attached to the proper place on a human body to measure the oscillation rate of that part. Fig. 7b shows a tag attached to a finger.

Computer: We use a Dell XPS8500 desktop with Intel Core i7 CPU of 3.4 GHz to process phase values collected by the reader.

VI. Evaluation

We conduct experiments to evaluate the performance of our system. The experiments are carried out in an office with a dimension of 166×102 feet^2. The office environment contains furniture including desks, chairs, paper boxes, desktop and small appliances. We invite four volunteers to emulate hand tremor in our experiments. The volunteers tremble their hands at different rates in the range of 2 *tps* to 6 *tps*. Each volunteer attaches one tag to one of his/her fingers for hand tremor rate measurement. Experiments are performed under different static/moving settings with a varying number of participants. Each experiment is repeated for 80 times to produce average results. The true oscillation rates are counted visually during measurement by another person. The estimated rates are compared with the true rates for error measurement. No previous health-monitoring systems are designed for measuring the hand tremor rate using RF signals.

A. Hand Tremor Rate of One Static Person

Our first set of experiments use our system to measure the hand tremor rate of a single person who sits still in the office. The measurement results are given in Fig 8.

Fig. 8a compares the measured tremor rate and the true tremor rate. Each point in the plot represents one experimental measurement, where the x coordinate is the true tremor rate and the y coordinate is the measured tremor rate. The equality line, $y = x$, is presented for reference: A point closer to the equality line is more accurate. We can see that most points are clustered around the equality line, demonstrating a good measurement accuracy of our system. Fig. 8b depicts the standard deviation of the measurement results when the hand tremor rate varies from 2 to 6 *tps*. All the points in Fig. 8a are placed in four bins, $[2, 3)$, ..., $[5, 6]$. We compute the average bias in each bin, which is represented by the distance between the center bar in each bin and the equality line. The distance between the top (bottom) bar and the center bar is the standard deviation. Overall, the average measurement error our system is about 0.11 *tps*, which is accurate enough for most practical applications. Fig. 8c shows the cumulative density function (CDF) of the measurement error of hand tremor rate. For example, the 90 percentile of the measurement error is less than 0.3 *tps*. In conclusion, our system can yield very accurate measurement results of hand tremor rate for a single static person.

B. Hand Tremor Rate of One Moving Person

The second set of experiments use our system to measure the hand tremor rate when the person under monitoring is moving around in the office. Fig. 9a presents the experimental results of measuring the hand tremor rate of a moving

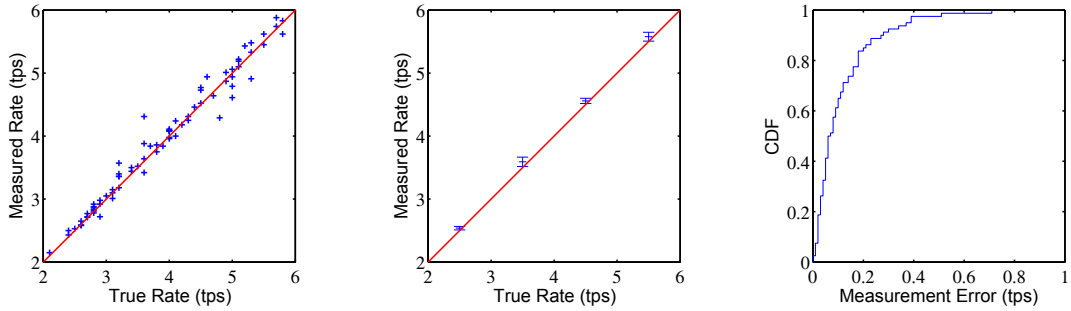

(a) measured oscillation rate (b) mean and standard deviation (c) CDF of measurement error

Fig. 8: Measurement accuracy of hand tremor rate of a single static person.

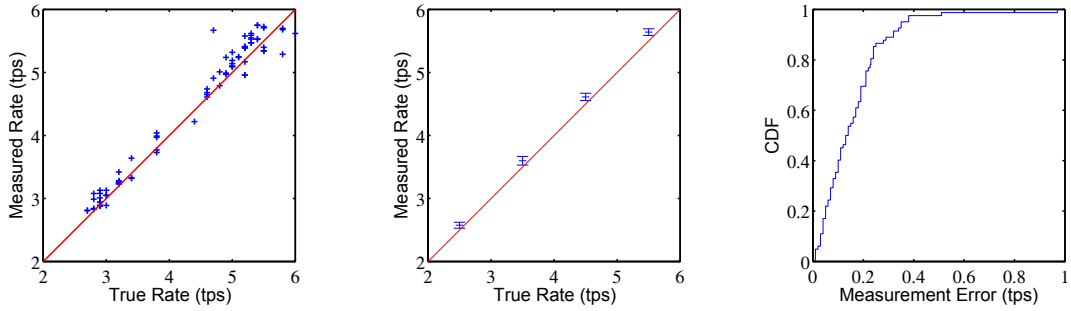

(a) measured oscillation rate (b) mean and standard deviation (c) CDF of measurement error

Fig. 9: Measurement accuracy of hand tremor rate of a single moving person.

number of people	average error	standard deviation
2	0.129	0.103
3	0.127	0.105
4	0.142	0.116

TABLE I: Measurement accuracy of hand tremor rates (in *tps*) of multiple static persons

number of people	average error	standard deviation
2	0.208	0.322
3	0.232	0.374
4	0.259	0.420

TABLE II: Measurement accuracy of hand tremor rates (in *tps*) of multiple moving persons

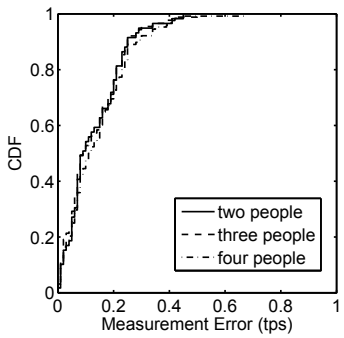

Fig. 10: Multiple static persons.

person. Again, most points cluster close to the equality line, demonstrating good performance. The measurement accuracy in terms of mean and standard deviation is presented in Fig. 9b. The average measurement error is 0.12 *tps*, which is slightly larger than that of the static-person case in Section VI-A. Besides, the CDF of the estimation error is presented in Fig. 9c, where the 90 percentile of the error is less than 0.3 *tps*. These results demonstrate that the proposed system can accurately measure the hand tremor rate under the more challenging scenario where the person is moving.

C. Hand Tremor Rates of Multiple Static Persons

The third set of experiments use our system to measure the hand tremor rates of multiple static persons. We conduct experiments with 2, 3, and 4 volunteers, respectively, each with a tag attached to a finger.

Table I presents the mean errors and the standard deviations. In the second column, the mean measurement errors are 0.129, 0.127 and 0.142 *tps* for two, three and four persons, respectively. It shows that the mean error is not very sensitive to the number of persons under monitoring. In the third column, the

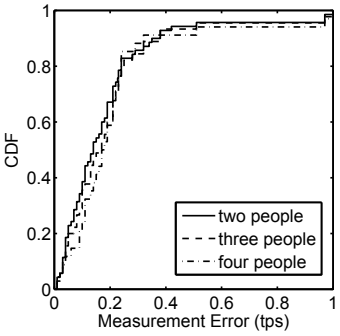

Fig. 11: Multiple moving persons.

standard deviations are 0.103, 0.105 and 0.116, respectively; they are not very sensitive to the number of persons, either. The reason is that the collision-resolving arbitration protocol allows the reader to interrogate each tag individually and record its phase values based on its ID. Consequently, our system can measure the oscillation rate on each tag without interference. Fig. 10 presents the CDF of the measurement error. For example, the 90 percentile of measurement error is less than 0.3 *tps* when four people are monitored simultaneously.

D. Hand Tremor Rates of Multiple Moving Persons

The fourth set of experiments evaluate the performance of our system for measuring hand tremor rates of 2, 3, or 4 moving persons simultaneously. The results are shown in Table II, where the mean measurement errors are 0.208, 0.232 and 0.259 *tps* (in the second column) for 2, 3 and 4 persons, respectively. They are only slightly larger than the results in Table I for the static case. The standard deviations of the error are presented in the third column; they are all small. Fig. 11 shows the CDF of the measurement error. The 90 percentile of measurement error is about 0.4 *tps* when four people are monitored simultaneously.

VII. Conclusion

In this paper, we design a novel wireless health-monitoring system using RFID tags. It provides a general and effective way of measuring oscillation rates. More specifically, the system uses the fine-grained phase values reported by an off-the-shelf RFID reader to estimate the oscillation rate of a human body with great accuracy. The design supports the measurement of hand tremor rate of one person or the measurement of multiple persons simultaneously, even when the individuals move around, which represents a significant improvement over the previous systems. We have implemented a prototype and performed extensive experiments. Our experimental results demonstrate the effectiveness of our system in providing accurate rate measurements under challenging settings.

VIII. Acknowledgements

This work was in part supported by the National Science Foundation under grants CNS-1409797 and CNS-1718708.

References

[1] C. A. Kushida, M. R. Littner, T. Morgenthaler, C. A. Alessi *et al.*, "Practice parameters for the indications for polysomnography and related procedures: an update for 2005," *Sleep*, vol. 28, no. 4, pp. 499–521, 2005.

[2] S. Patel, B. Chen, T. Buckley, R. Rednic, D. McClure, D. Tarsy, L. Shih, J. Dy, M. Welsh, and P. Bonato, "Home Monitoring of Patients with Parkinsons Disease via Wearable Technology and a Web-based Application," *IEEE EMBC*, 2010.

[3] G. Albani, G. Sandrini, G. Kunig, and K. L. Leenders, "Differences in the EMG pattern of lea muscle activation during locomotion in Parkinsons disease," *Funct. Neurol*, vol. 18, pp. 165 – 170, 2003.

[4] N. Patwari, L. Brewer, Q. Tate, O. Kaltiokallio, and M. Bocca, "Breathfinding: A wireless network that monitors andlocates breathing in a home," *IEEE Journal of Selected Topics in Signal Processing*, vol. 8, no. 1, pp. 30–42, 2014.

[5] J. Liu, Y. Wang, Y. Chen, J. Yang, X. Chen, and J. Cheng, "Tracking Vital Signs During Sleep Leveraging Off-the-shelf WiFi," *Proc. of ACM MobiHoc*, 2015.

[6] F. Adib, H. Mao, Z. Kabelac, D. Katabi, and R. C. Miller, "Smart Homes that Monitor Breathing and Heart Rate," *Proc. of ACM CHI*, 2015.

[7] H. Abdelnasser, K. A. Harras, and M. Youssef, "UbiBreathe: A Ubiquitous non-Invasive WiFi-based Breathing Estimator," *Proc. of ACM MobiHoc*, 2015.

[8] H. Wang, D. Zhang, J. Ma, Y. Wang, Y. Wang, D. Wu, T. Gu, and B. Xie, "Human Respiration Detection with Commodity WiFi Devices: Do User Location and Body Orientation Matter?" *Proc. of ACM Ubicomp*, 2016.

[9] D. Halperin, W. Hu, A. Sheth, and D. Wetherall, "Tool release: gathering 802.11 n traces with channel state information," *Proc. of ACM SIGCOMM Computer Communication Review*, vol. 41, no. 1, pp. 53–53, 2011.

[10] L. Yang, Y. Chen, X. Li, C. Xiao, M. Li, and Y. Liu, "Tagoram: real-time tracking of mobile RFID tags to high precision using cots devices," *Proc. of ACM MobiCom*, 2014.

[11] L. Yang, Q. Lin, X. Li, T. Liu, and Y. Liu, "See Through Walls with COTS RFID System," *Proc. of ACM MobiCom*, 2015.

[12] Y. Hou, Y. Wang, and Y. Zheng, "TagBreathe: Monitor Breathing with Commodity RFID Systems," *Proc. of IEEE ICDCS*, 2017.

[13] J. Liu, Y. Zhang, M. Chen, S. Chen, and L. Chen, "Collision-resistant Communication Model for Stateless Networked Tags, poster paper," *Proc. of IEEE ICNP*, 2016.

[14] Y. Zhang, S. Chen, Y. Zhou, and Y. Fang, "Anonymous Temporal-Spatial Joint Estimation at Category Level over Multiple Tag Sets," *Proc. of IEEE INFOCOM*, 2018.

[15] Y. Zhang, S. Chen, Y. Zhou, and O. Odegbile, "Missing-Tag Detection With Presence of Unknown Tags," *Proc. of IEEE SECON*, 2018.

[16] M. Chen, S. Chen, Y. Zhou, and Y. Zhang, "Identifying State-free Networked Tags," *IEEE/ACM Transactions on Networking*, 2017.

[17] "ImpinJ," *http://www.impinj.com/*.

[18] T. Hao, G. Xing, and G. Zhou, "isleep: unobtrusive sleep quality monitoring using smartphones," *Proc. of ACM Sensys*, 2013.

[19] A. Tzallas, M. Tsipouras, G. Rigas, D. G. Tsalikakis *et al.*, "PERFORM: A System for Monitoring, Assessment and Management of Patients with Parkinsons Disease," *Sensors*, vol. 14, p. 21329 C 21357, 2014.

[20] T. Ballal, R. B. Shouldice, C. Heneghan, , and A. Zhu, "Tracking Vital Signs During Sleep Leveraging Off-the-shelf WiFi," *IEEE BioWireless*, 2012.

[21] A. Lazaro, D. Girbau, and R. Villarino, "Analysis of vital signs monitoring using an IR-UWB radar," *Progress In Electromagnetics Research*, 2010.

[22] L. Yang, Y. Li, Q. Lin, X. Li, and Y. Liu, "Making Sense of Mechanical Vibration Period with Sub-millisecond Accuracy Using Backscatter Signals," *Proc. of ACM MobiCom*, 2016.

[23] "EPC Radio-Frequency Identity Protocols Class-1 Gen-2 UHF RFID Protocol for Communications at 860MHz-960MHz, EPCglobal," *http://www.epcglobalinc.org/uhfclg2*.

[24] M. Wachowiak, G. Rash, P. Quesada, and A. Desoky, "Comparison of Wavelet-Based and Tradidional Noise Removal Techniques," *Gait and Biomechanics Laboratory, University of Louisville*, August 1998.

[25] "Laird," *http://www.lairdtech.com/products/s9028PCL*.

[26] "AlienTags," *http://www.alientechnology.com/products/tags/squiggle/*.